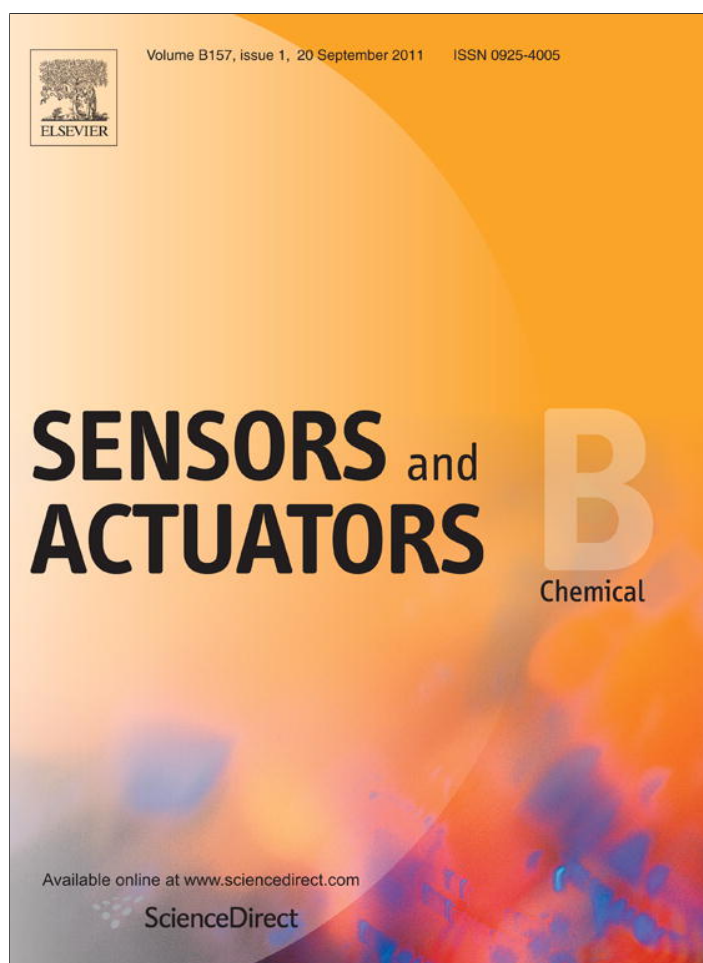


Provided for non-commercial research and education use.  
Not for reproduction, distribution or commercial use.



This article appeared in a journal published by Elsevier. The attached copy is furnished to the author for internal non-commercial research and education use, including for instruction at the authors institution and sharing with colleagues.

Other uses, including reproduction and distribution, or selling or licensing copies, or posting to personal, institutional or third party websites are prohibited.

In most cases authors are permitted to post their version of the article (e.g. in Word or Tex form) to their personal website or institutional repository. Authors requiring further information regarding Elsevier's archiving and manuscript policies are encouraged to visit:

<http://www.elsevier.com/copyright>



Contents lists available at ScienceDirect

## Sensors and Actuators B: Chemical

journal homepage: [www.elsevier.com/locate/snb](http://www.elsevier.com/locate/snb)Enhanced H<sub>2</sub>S sensing characteristics of Pt doped SnO<sub>2</sub> nanofibers sensors with micro heaterKi-Young Dong<sup>a</sup>, Joong-Ki Choi<sup>b</sup>, In-Sung Hwang<sup>b</sup>, Jin-Woo Lee<sup>c</sup>, Byung Hyun Kang<sup>a</sup>, Dae-Jin Ham<sup>a</sup>, Jong-Heun Lee<sup>b</sup>, Byeong-Kwon Ju<sup>a,\*</sup><sup>a</sup> Display and Nanosystem Laboratory, College of Engineering, Korea University, Seoul 136-713, Republic of Korea<sup>b</sup> Department of Materials Science and Engineering, College of Engineering, Korea University, Seoul 136-713, Republic of Korea<sup>c</sup> Department of Biomedical Engineering, College of Medicine, Kyung Hee University, Seoul 130-701, Republic of Korea

## ARTICLE INFO

## Article history:

Received 28 October 2010

Received in revised form 21 January 2011

Accepted 20 March 2011

Available online 26 March 2011

## Keywords:

SnO<sub>2</sub> nanofibers

Micro heater

Gas sensors

Pt–SnO<sub>2</sub>H<sub>2</sub>S sensors

## ABSTRACT

Gas sensors were designed and fabricated using oxide nanofibers as the sensing materials on micro platforms using micromachining technology. Pure and Pt doped SnO<sub>2</sub> nanofibers were prepared by electrospinning and their H<sub>2</sub>S gas sensing characteristics were subsequently investigated. The sensing temperatures of 300 and 500 °C could be attained at the heater powers of 36 and 94 mW, respectively, and the sensors showed high and fast responses to H<sub>2</sub>S. The responses of 0.08 wt% Pt doped SnO<sub>2</sub> nanofibers to 4–20 ppm H<sub>2</sub>S, were 25.9–40.6 times higher than those of pure SnO<sub>2</sub> nanofibers. The gas sensing characteristics were discussed in relation to the catalytic promotion effect of Pt, nano-scale morphology of electrospun nanofibers, and sensor platform using micro heater.

© 2011 Elsevier B.V. All rights reserved.

## 1. Introduction

The development of gas sensors has received considerable attention in recent years, especially in the monitoring of environmental pollution. It is well known that performance of gas sensors are regulated by their sensitivity, selectivity, response/recovery speed, stability, and reproducibility [1–3].

Semiconducting metal oxide such as SnO<sub>2</sub>, ZnO, In<sub>2</sub>O<sub>3</sub>, ZrO<sub>2</sub>, CeO<sub>2</sub>, WO<sub>3</sub>, and TiO<sub>2</sub> are the most common materials used for gas sensors [4–7]. Among these oxides, SnO<sub>2</sub> has been one of the more promising materials used for gas sensors. Recently, interest in one-dimensional (1D) nano-structured SnO<sub>2</sub> with a high surface to volume ratio has attracted special attention [8–13]. Therefore, the development of oxide materials with 1D geometry is highly desirable. Considerable efforts have been made to fabricate 1D oxide SnO<sub>2</sub> nanowires, nanofibers and nanorods using metal organic chemical vapor deposition, chemical vapor deposition, thermal oxidation, thermal evaporation condensation, self-catalytic growth, molten salt synthesis, and electrospinning [9–14]. Each method produces 1D sensor elements that can be

incorporated into a variety of sensor platforms. In particular, electrospun nanofibers with a high surface to volume ratio and a less-agglomerated configuration offer a potential application to gas sensors.

Hydrogen sulfide (H<sub>2</sub>S) is a corrosive, colorless, toxic, and flammable gas, occurring naturally in crude petroleum, natural gas, volcanic gases, and hot springs with smell of rotten eggs. It can also be produced from industrial activities that include food processing, coking ovens, craft paper mills, tanneries, and petroleum refineries [15]. To date, various semiconductor gas sensors have been employed to detect trace concentrations of H<sub>2</sub>S, including those that use SnO<sub>2</sub>, CuO-doped SnO<sub>2</sub>, and In<sub>2</sub>O<sub>3</sub> [16–18]. It should be noted that the H<sub>2</sub>S sensors found in the literature often show slow or irreversible recovery reactions. This hampers the application of H<sub>2</sub>S sensors to commercial enterprises. From the viewpoint of applications, a small size and low power consumption are other important issues, which can be best accomplished when the micromachining technology is applied to the fabrication of a micro-heater and microelectrodes.

In this study, we fabricate pure and 0.08 wt% Pt doped SnO<sub>2</sub> nanofiber sensors on micro heater platforms in order to achieve low power consumption and then investigated the H<sub>2</sub>S sensing characteristics. The focus of the study is placed upon the minimization of the power consumption by using micro-heater and the enhancement of gas response and the response/recovery kinetics by the addition of Pt catalyst on electrospun SnO<sub>2</sub> nanofibers.

\* Corresponding author at: Department of Electrical Engineering, Korea University, Anam-Dong, Sungbuk-Gu, Seoul 136-713, Korea. Tel.: +82 2 3290 3237; fax: +82 2 3290 3791.

E-mail address: [bkju@korea.ac.kr](mailto:bkju@korea.ac.kr) (B.-K. Ju).

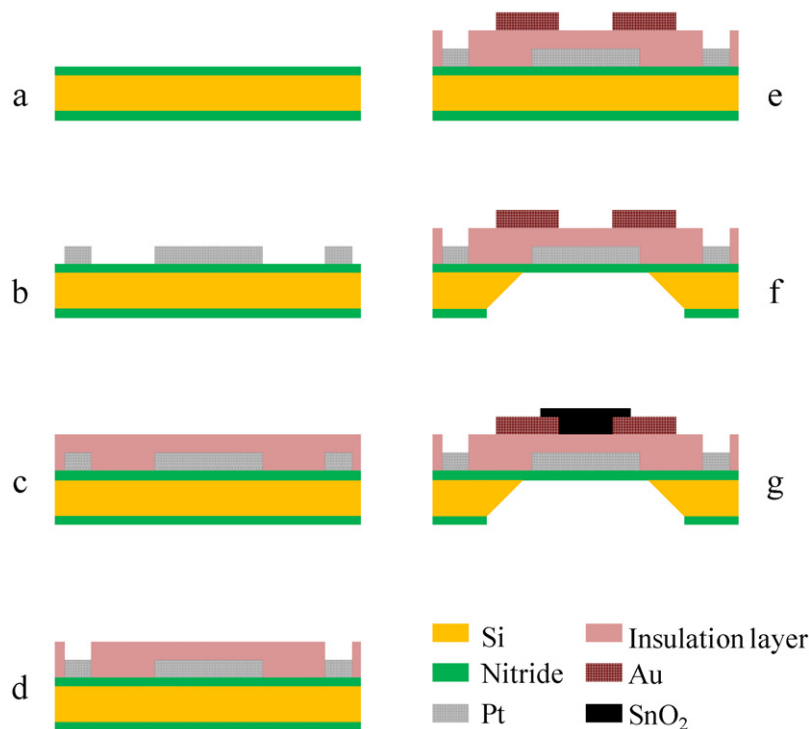


Fig. 1. The fabrication process of the micro heater based gas sensor.

## 2. Experimental

### 2.1. Sensor fabrication process

The fabrication process used for our sensor is shown in Fig. 1. The sensor integrated with Pt micro-heater was fabricated on double-side polished p-type Si wafer (thickness: 500  $\mu\text{m}$ ), and all of the patterning processes were performed by photolithography. The electrodes have a width of 10  $\mu\text{m}$  with gap size of 10  $\mu\text{m}$  and thickness of 320 nm. Electrical insulating layers are stacked between the electrodes and the micro heater. The layers consist of  $\text{SiO}_2/\text{Si}_3\text{N}_4/\text{SiO}_2$  structure. The silicon substrate was etched away by using an anisotropic etchant (KOH) to achieve the thermal isolation on the substrate.

The details of our process are as follows: (1) a 2  $\mu\text{m}$  thick  $\text{Si}_3\text{N}_4$  layer was deposited on a p-type double-sided polished silicon wafer by low pressure chemical vapor deposition (LPCVD); (2) a 20/300 nm Ti/Pt layer was deposited on the electrical insulator by E-beam evaporator. The Ti/Pt micro heater was patterned by photo lithography and then etched by inductive coupled plasma (ICP) etching. (3) a 1  $\mu\text{m}$   $\text{SiO}_2/\text{Si}_3\text{N}_4/\text{SiO}_2$  thin film used as an electrical insulating layer was deposited on the Pt micro heater by plasma enhanced chemical vapor deposition (PECVD). The deposited insulation layer was patterned and then etched by reactive ion etching (RIE) method to make the contact space for the Pt micro heater. (4) a 320 nm Cr/Au thin film was patterned to make the bonding pads and the pair of electrodes for the sensing layer by lift-off technique; (5) a square window pattern was opened in the  $\text{Si}_3\text{N}_4$  on the silicon wafer backside by photolithography and etched by RIE. The silicon substrate was etched away by using an anisotropic etchant (KOH) to achieve the thermal isolation on the substrate. An optical image of the fabricated micro gas sensor is shown in Fig. 2(a). Fig. 2(b) indicates the variation of the sensor temperature as a function of the power dissipated by the Pt micro heater. At the temperature of 600  $^\circ\text{C}$ , the micro heater with a thermally insulated dielectric diaphragm consumed a power of 124 mW. A thinner and narrower

silicon membrane may reduce the heater loss due to the conduction and convection, which are related to the area of the silicon diaphragm and the distance between the silicon diaphragm and chip frame, respectively.

### 2.2. Electrospinning setup and process

Pure  $\text{SnO}_2$  and Pt-doped  $\text{SnO}_2$  nanofibers were synthesized via the electrospinning process [19]. 1 g of  $\text{SnCl}_2 \cdot 2\text{H}_2\text{O}$  (98 + %, Acros Organics, Belgium) was dissolved in 17 g of mixed solvents consisting of ethanol (99.9%, J. T. Baker Chemical Co., Ltd., USA) and N, N-dimethylformamide (99.5%, Samchun Chemical Co., Ltd., Korea) (ethanol: N, N-dimethylformamide = 1:1 by wt%) and stirred for 2 h. Then 2 g of polyvinylpyrrolidone (Mw = 1,300,000, Sigma-Aldrich Co., Ltd., USA) was added to the solution. After stirring for 10 h, a clear solution was attained, which was used for the preparation of pure  $\text{SnO}_2$  nanofibers. For the preparation of Pt doped  $\text{SnO}_2$  nanofibers, the corresponding amount of  $\text{PtCl}_4$  (98%, Sigma-Aldrich Co., Ltd., USA) was added to the solution. ( $\text{Pt}/\text{SnO}_2 = 0.08$  wt%) The solution was loaded in a plastic syringe and electrospun by applying 20 kV at an electrode distance of 10 cm. The as-spun fibers were heat-treated at 600  $^\circ\text{C}$  for 2 h to convert into  $\text{SnO}_2$  or 0.08 wt% Pt doped  $\text{SnO}_2$  nanofibers.

The nanofibers were dispersed in isopropanol (Sigma-Aldrich Co., Ltd., USA) by ultrasonic treatment and subsequently dried at 80  $^\circ\text{C}$  for 24 h. The pristine and Pt doped  $\text{SnO}_2$  nanofibers were mixed with organic binders (ethyl cellulose:  $\alpha$ -terpinol = 1: 14 by wt%), respectively and printed on the substrates with finger Au electrodes and a Pt micro heater.

### 2.3. Gas sensor measurements

The gas sensing characteristic were measured using a flow test system. The gas concentration was controlled by changing the mixing ratio of the dry parent gases (20 ppm  $\text{H}_2\text{S}$  in air balance) to dry synthetic air. The sensor responses are usually reported in terms

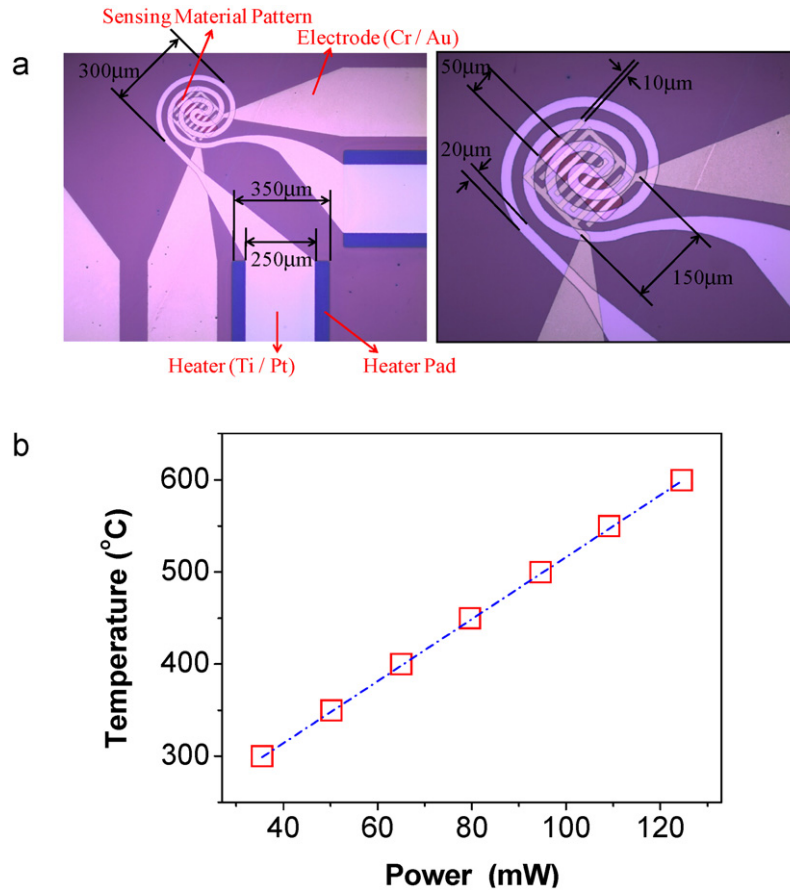


Fig. 2. (a) Images of the fabricated gas sensors (b) the sensor heater temperature as a function of the applied heater power.

of the ratio of the electrical resistance, to the gas response ( $R_a/R_g$ ), where  $R_a$  and  $R_g$  are the electrical resistance of the sensor upon exposure to dry air and  $H_2S$  vapor, respectively. The changes in resistance of  $SnO_2$  were automatically measured using LabVIEW software and KEITHLEY 2400 source meter.

### 3. Results and discussion

The pure and Pt doped Sn-precursor nanofibers showed amorphous X-ray diffraction (XRD) patterns regardless of composition (data not shown). The XRD patterns observed for pure  $SnO_2$  and 0.08 wt% Pt doped  $SnO_2$  nanofibers after heat treatment at 600 °C for 2 h in air are shown in Fig. 3. All the specimens showed a  $SnO_2$  rutile structure (JCPDS # 77-0447). However, Pt peaks are not observed in XRD patterns probably due to the Pt concentrations being low.

Fig. 4 shows the SEM images of the as-spun precursor nanofibers and pure  $SnO_2$  and 0.08 wt% Pt doped  $SnO_2$  nanofibers after heat treatment at 600 °C for 2 h. The as-spun Sn and Pt-Sn composite fibers showed clean surface morphologies and exhibited a range of diameters from 200 to 300 nm (Fig. 4(a)–(d)). Fig. 4(e)–(h) shows the surface of the  $SnO_2$  and 0.08 wt% Pt doped  $SnO_2$  nanofibers after being annealed at 600 °C for 2 h. Note that the surface becomes rougher from the heat treatment. The diameter of 0.08 wt% Pt- $SnO_2$  nanofibers (~120 nm, Fig. 4(g) and (h)) is significantly smaller than that of pure  $SnO_2$  nanofibers (~300 nm, Fig. 4(e) and (f)). The cause of the thinning of the Pd doped nanofibers is unclear at this moment and need to be studied further. However, the change of chemistry in the source solution used for electrospinning by the addition of Pt source materials can be considered to be a possibility. The primary particle sizes within the nanofibers are 39 and 41 nm,

respectively. The size decrease in the primary in Pt-doped  $SnO_2$  nanofibers may be attributed to the retardation of the grain growth of  $SnO_2$  particles due to the presence of the secondary Pt nanoparticle. The decrease of the nanofiber diameter and nanoparticle size

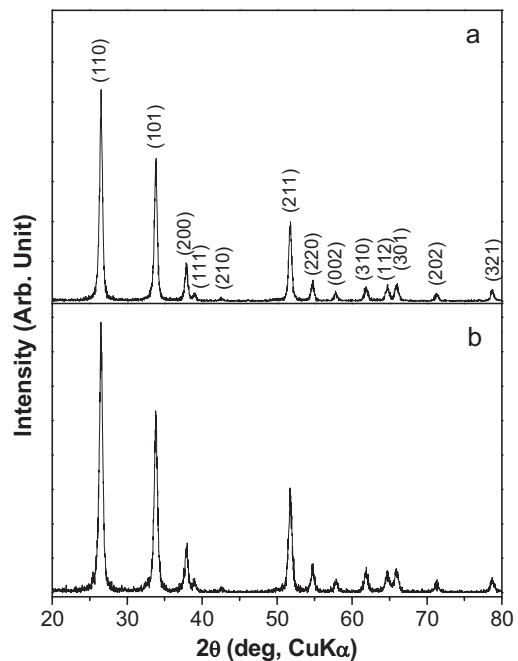
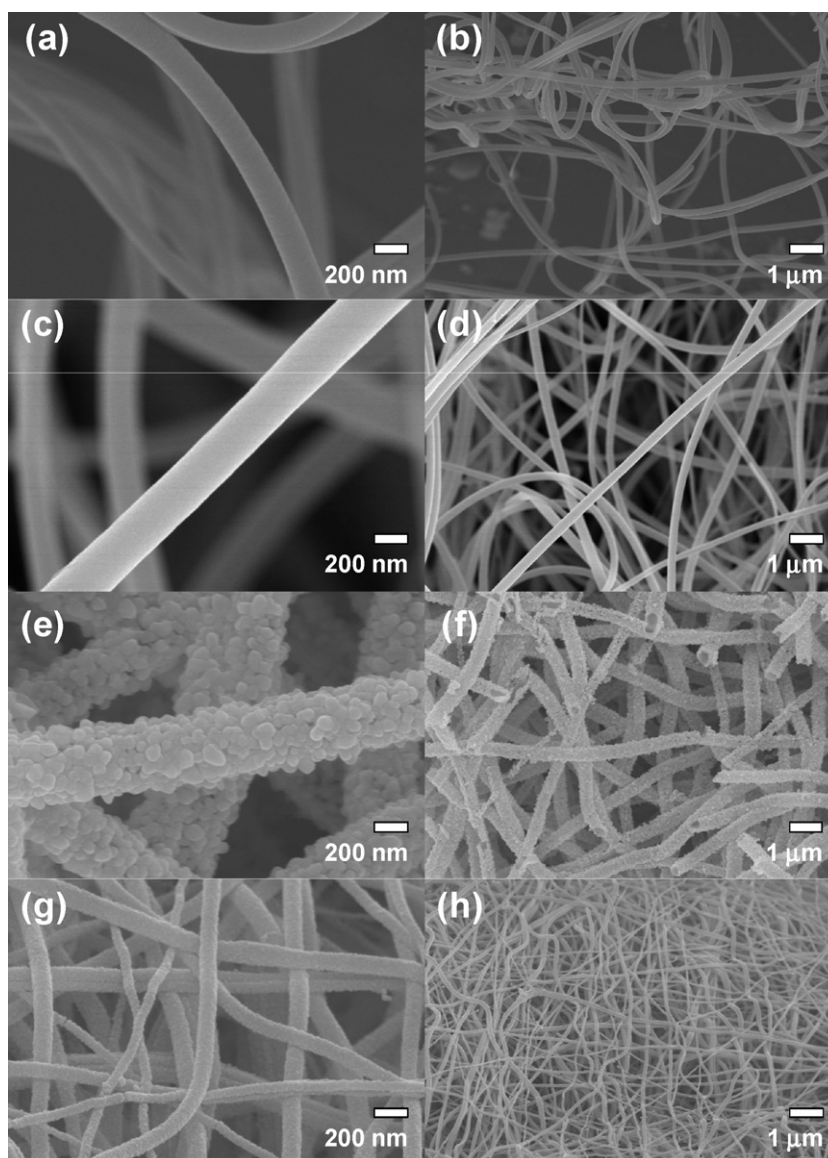


Fig. 3. X-ray diffraction (XRD) patterns of (a) pure  $SnO_2$ , (b) 0.08 wt% Pt- $SnO_2$  nanofibers heat-treated at 600 °C for 2 h.





**Fig. 4.** Scanning electron microscopy (SEM) images of (a) and (b) as-spun pure  $\text{SnO}_2$  nanofibers, (c) and (d) 0.08Pt-doped  $\text{SnO}_2$  nanofibers, (e) and (f) pure  $\text{SnO}_2$  nanofibers after heating at  $600^\circ\text{C}$  for 2 h. (g) and (h) 0.08Pt-doped  $\text{SnO}_2$  nanofibers after heating at  $600^\circ\text{C}$  for 2 h.

will contribute to the enhancement of the gas sensing behaviors (Fig. 5).

The dynamic sensing transients to 4–20 ppm  $\text{H}_2\text{S}$  of the sensors  $300\text{--}500^\circ\text{C}$  are shown in Fig. 6. The resistance decreases upon exposure to  $\text{H}_2\text{S}$ , corresponding to a typical n-type semiconducting behavior. In all of the sensors, the sensor signal was very stable and reversible even after repeated exposures to  $\text{H}_2\text{S}$ , which indicates that these nanofiber sensors fabricated onto the micro heater can reliably detect trace concentrations of  $\text{H}_2\text{S}$ . It should be noted that the variations of resistance upon exposure to  $\text{H}_2\text{S}$  of 0.08 wt% Pt doped  $\text{SnO}_2$  sensors (Fig. 6(d–f)) are significantly higher than those of pure  $\text{SnO}_2$  nanofiber sensors. Wan et al. also fabricated MEMS based gas sensor using pure and doped oxide materials [20,21]. The response time reported in the references is about 1–2 s which is similar to the response time of our  $\text{SnO}_2$  nanofiber sensors. Such similarity may be attributed to the porosity of the nanofibers.

The response time against temperature was also investigated in range of  $300\text{--}500^\circ\text{C}$ . The  $\text{H}_2\text{S}$  responses were calculated from the sensor transients and the results were summarized in Fig. 7(a)

and (d). In pure  $\text{SnO}_2$  nanofiber sensors, the responses to 4–20 ppm  $\text{H}_2\text{S}$  ranged from 23 to 121 at  $300^\circ\text{C}$ . The responses tended to decrease when increasing the sensor temperature up to  $500^\circ\text{C}$  (Fig. 7(a)). Due to the doping of 0.08 wt% Pt to  $\text{SnO}_2$  nanofibers, the gas responses to 4–20 ppm  $\text{H}_2\text{S}$  were increased to 800–5100, which correspond to 25.9–40.6-fold increase (Fig. 7(d)).

The modification of the surface conditions by the introduced additives generates different electrical characteristics due to the variations of the grain barriers. Fig. 6 shows the Pt doped  $\text{SnO}_2$  nanofiber higher resistance, which indicates a higher grain barrier. This increase in the grain barrier may be due to a higher oxygen adsorption at the grain surface enhanced by a higher density of the semiconductor surface adsorption sites introduced by the presence of the additive, or may be directly related to the presence of the Pt catalyst localized at the grain surface [22,23]. Pt is known to promote the gas sensing reaction by the spill-over of sample gas (chemical sensitization), whereas Pd is known to promote the gas sensing reaction by electronic interaction between Pd and sensing materials (electronic sensitization) [24]. Thus, the  $R_a$  value usually becomes very high in the case of chemical sensitization. In

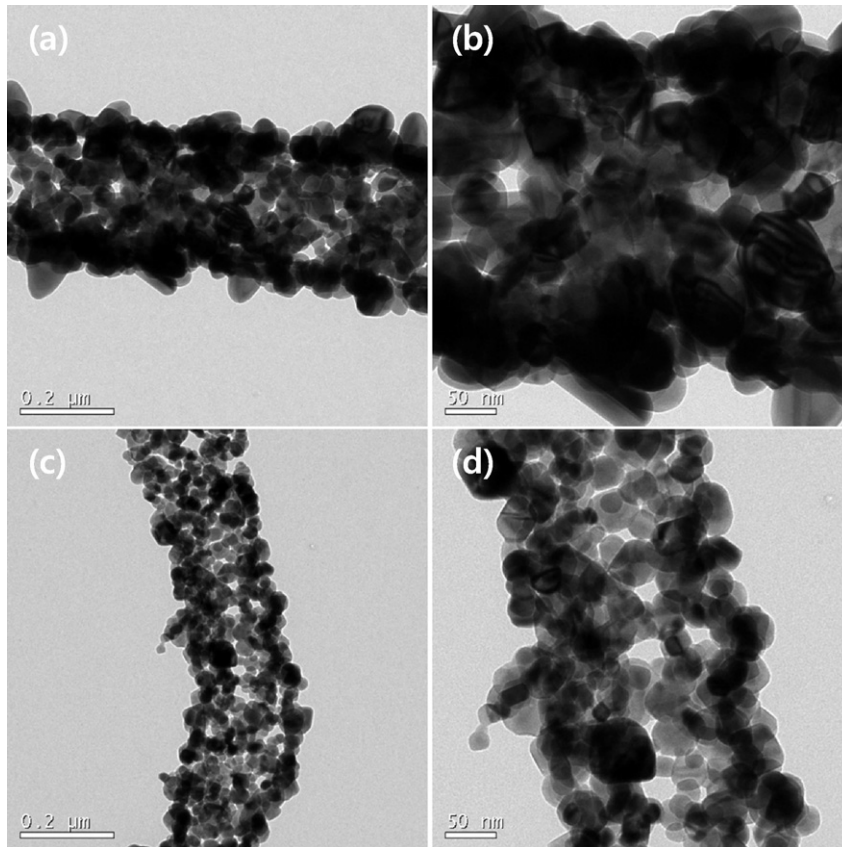


Fig. 5. Transmission electron microscopy (TEM) images of (a) and (b) pure SnO<sub>2</sub>, (c) and (d) 0.08Pt-doped SnO<sub>2</sub> nanofibers heat-treated at 600 °C for 2 h.

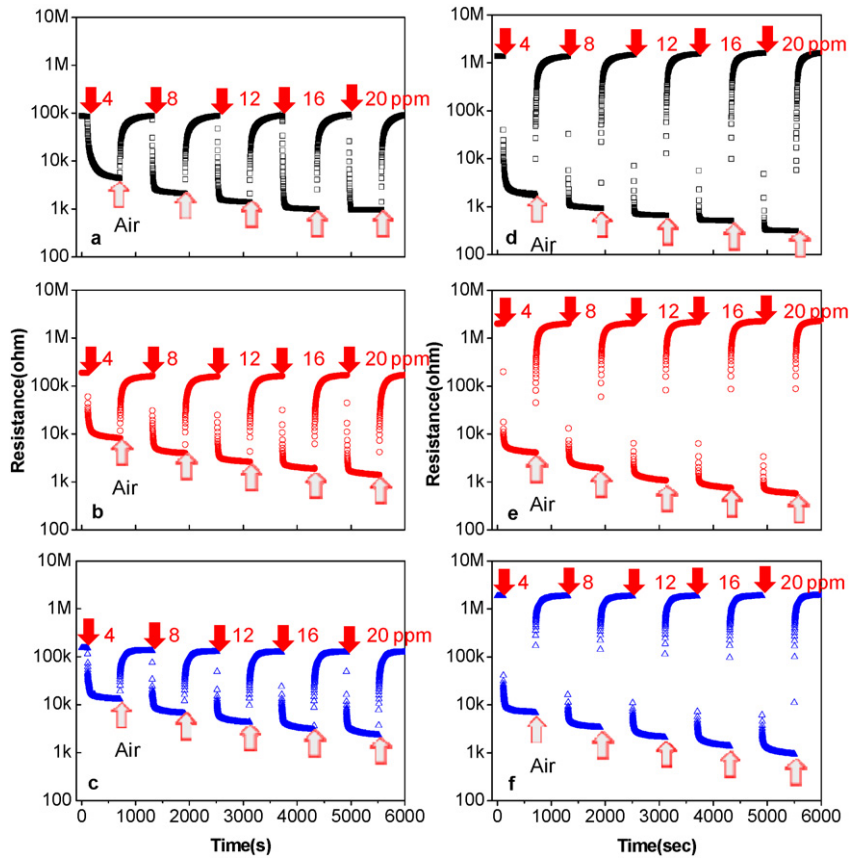
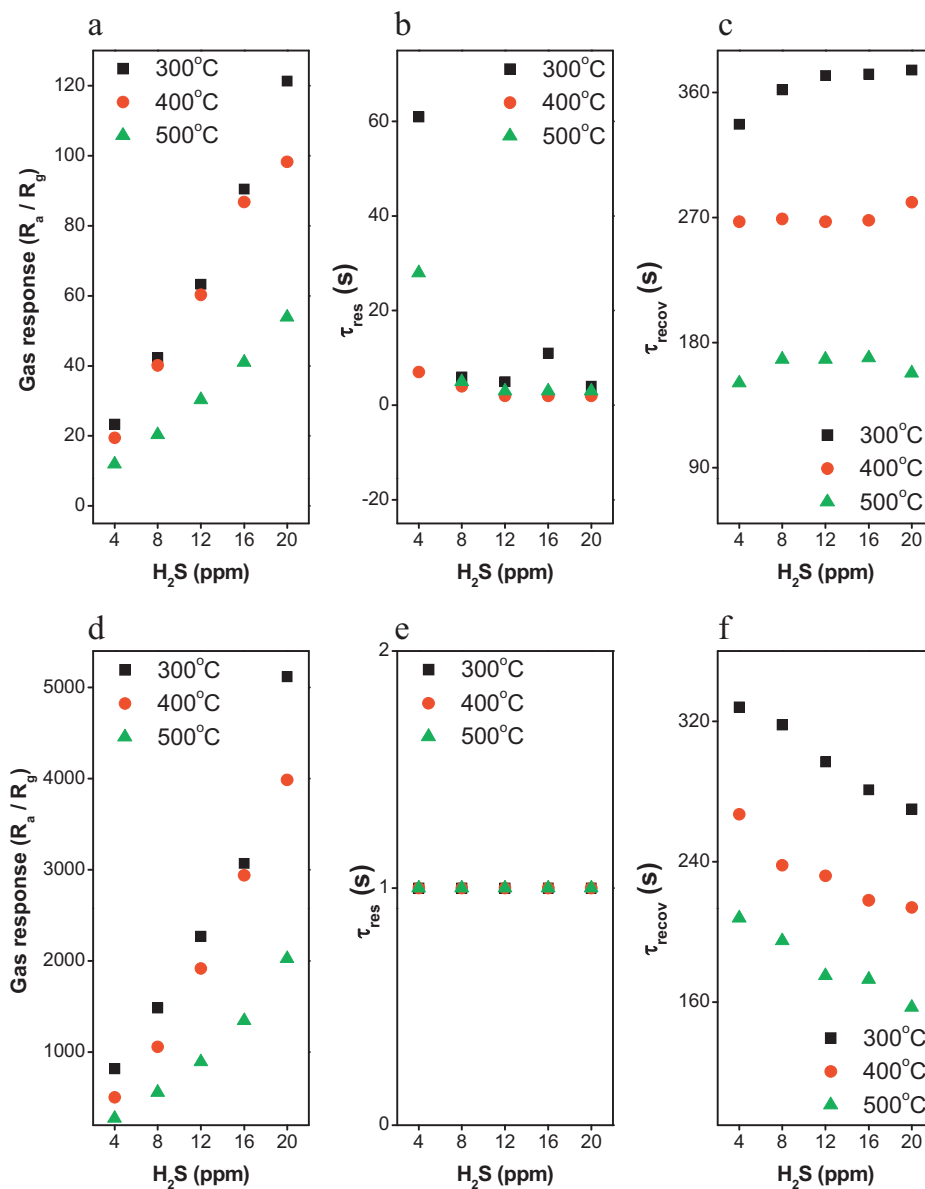


Fig. 6. Response of the various H<sub>2</sub>S concentration gas sensing transients: (a) pure SnO<sub>2</sub> sensor, T=300 °C; (b) pure SnO<sub>2</sub> sensor, T=400 °C; (c) pure SnO<sub>2</sub> sensor, T=500 °C; (d) 0.08Pt-SnO<sub>2</sub> sensor, T=300 °C; (e) 0.08Pt-SnO<sub>2</sub> sensor, T=400 °C; (f) 0.08Pt-SnO<sub>2</sub> sensor, T=500 °C.



**Fig. 7.** (a) Gas responses for pure  $\text{SnO}_2$  sensor ( $R_a/R_g$ ) (b) 90% response times ( $\tau_{\text{res-90}}$ ) at the sensing temperature of 300–500 °C, and (c) 90% recovery times ( $\tau_{\text{recov-90}}$ ) at the sensing temperature of 300–500 °C. (d) Gas responses for 0.08Pt- $\text{SnO}_2$  sensor, (e) 90% response times ( $\tau_{\text{res-90}}$ ) at the sensing temperature of 300–500 °C, and (f) 90% recovery times ( $\tau_{\text{recov-90}}$ ) at the sensing temperature of 300–500 °C.

Fig. 6, the  $R_a$  values of 0.08 wt% Pt doped  $\text{SnO}_2$  nanofiber sensors is  $\sim 10$  times higher than those of undoped  $\text{SnO}_2$  nanofiber sensors. Nevertheless, it is very difficult to explain the Pt-induced increase of  $R_a$  simply by the chemisorption between Pt and  $\text{SnO}_2$  if one considered the general agreement on the role of Pt as a chemical sensitizer. Instead, the increased contribution of electron depletion layer within single particle due to the Pt-induced decrease of primary particle size provides more reasonable explanation.

To investigate the response and recovery kinetics, the times to reach 90% variation in resistance upon exposure for  $\text{H}_2\text{S}$  and air were defined as 90% response time ( $\tau_{\text{res}}$ ) and 90% recovery time ( $\tau_{\text{recov}}$ ), respectively, and these values were calculated from the sensing transients. The  $\tau_{\text{res}}$  and  $\tau_{\text{recov}}$  values calculated at the sensing temperature of 300–500 °C were given in Fig. 7.

In all of the sensors, the  $\tau_{\text{res}}$  values were very short ( $<10$  s), indicating that both the in-diffusion of the analyte gas and its oxidation with the negatively charged surface oxygen occur quickly. The fast gas diffusion in the present study was attributed to the less agglomerated configuration of the 1-D nanofibers (Fig. 5).

The  $\tau_{\text{res}}$  values of 0.08 wt% Pt doped  $\text{SnO}_2$  nanofiber sensor (1 s) were significantly shorter than those of undoped  $\text{SnO}_2$  nanofiber sensors (2–7 s) (Fig. 7(e)), demonstrating the high and fast response of the 0.08 wt% Pt doped  $\text{SnO}_2$  nanofibers sensors. Considering that both the undoped and Pt-doped nanofibers sensors have the less-agglomerated configuration needed for easy gas diffusion, the increase of the response speed caused by the Pt doping can be explained by the promotion of the oxidation reaction between the  $\text{H}_2\text{S}$  and the negatively charged surface oxygen caused by the Pt catalyst.

In contrast, the recovery took a relatively long time in all of the sensors. Even at 400 °C, the  $\tau_{\text{recov}}$  values of the undoped  $\text{SnO}_2$  nanofibers sensor, ranged from 267 to 281 s. These values were much longer than the corresponding  $\tau_{\text{res}}$  values (2–7 s). As for 0.08 wt% Pt doped  $\text{SnO}_2$  nanofibers sensor, the  $\tau_{\text{recov}}$  values at similar conditions ranged from 214 s to 267 s. Although  $\tau_{\text{recov}}$  values were still much longer than the corresponding  $\tau_{\text{res}}$  values which saturated within 1 s (Fig. 7(e)), these values were shorter than the untreated  $\text{SnO}_2$  nanofibers sensors. These results

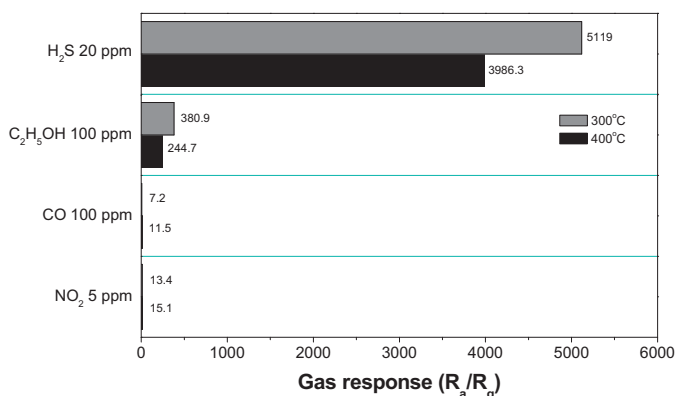


**Fig. 8.** Gas response ( $R_a/R_g$  or  $R_g/R_a$ ) of 0.08 wt% Pt-doped SnO<sub>2</sub> nanofibers to 20 ppm H<sub>2</sub>S, 100 ppm C<sub>2</sub>H<sub>5</sub>OH, 100 ppm CO, and 5 ppm NO<sub>2</sub> at 300 and 400 °C.

show that the Pt shortens both the response and the recovery times.

The responses at relatively high temperatures were mainly explored because of the reasonable recovery time of the sensor. Although our sensor displayed similar response towards H<sub>2</sub>S at lower temperature, below 300 °C, the recovery time was extremely long.

At 400 °C, although the response to 40 ppm H<sub>2</sub>S was decreased to 3986.3, it is still significantly higher than those of other gases. This shows that the selectivity detection of H<sub>2</sub>S with a minimal interference of C<sub>2</sub>H<sub>5</sub>OH, CO and NO<sub>2</sub> can be accomplished using 0.08 wt% Pt-doped SnO<sub>2</sub> nanofiber gas sensor (Fig. 8).

The responses to H<sub>2</sub>S in these sensors are significantly higher than those found in the literature and comparable to the highest values [25–27]. The high response and rapid response kinetics are mainly based on the 1D structure of the nanofibers and the Pt doping. The 1D nano-structures, with a large surface-to-volume ratio and a less-agglomerated configuration, and the catalytic promotion of the gas sensing reaction make them highly sensitive and efficient transducers of surface chemical processes into electrical signals.

#### 4. Conclusions

Pure and Pt-doped SnO<sub>2</sub> electrospun nanofibers were fabricated as gas sensors on micro heater and their H<sub>2</sub>S sensing characteristics were investigated. The fabricated micro platform gas sensors operated at below 36 mW at 300 °C. Compared to the pure SnO<sub>2</sub> nanofiber sensors, the Pt-doped SnO<sub>2</sub> nanofiber sensors exhibited better H<sub>2</sub>S gas sensing characteristics. The high gas response, and the fast responding and recovery kinetic in the Pt-doped SnO<sub>2</sub> nanofibers are explained by the catalytic promotion effect of the Pt and the less-agglomerated configuration of the nanofibers with a high surface area.

#### Acknowledgements

This work was supported by World Class University (WCU, R32-2009-000-10082-0) Project of the Ministry of Education, Science and Technology (Korea Science and Engineering Foundation) and partially supported by Basic Science Research Program through the National Research Foundation (NRF) of Korea funded by the Ministry of Education, Science and Technology (no.2009-0083126). This work of prof. J.-H. Lee was supported by KOSEF NRL program (no. ROA-2008-000-20032-0).

#### References

- [1] J. Kong, N. Franklin, C. Zhou, M. Chapline, S. Peng, K. Cho, H. Dai, Nanotube molecular wires as chemical sensors, *Science* 287 (2000) 622–625.
- [2] W. Gopel, K. Schierbaum, SnO<sub>2</sub> sensors current status and future prospects, *Sens. Actuators B* 26 (1995) 1–12.
- [3] Y. Yamada, Y. Seno, Y. Masuoka, K. Yamashita, Nitrogen oxides sensing characteristics of Zn<sub>2</sub>SnO<sub>4</sub> thin film, *Sens. Actuators B* 49 (1998) 248–252.
- [4] C. Rout, M. Hegde, C.N.R. Rao, H<sub>2</sub>S sensors based on tungsten oxide nanostructures, *Sens. Actuators B* 128 (2008) 488–493.
- [5] Y. Wang, Y. Wang, J. Cao, F. Kong, H. Xia, J. Zhang, B. Zhu, S. Wang, S. Wu, Low-temperature H<sub>2</sub>S sensors based on Ag-doped-Fe<sub>2</sub>O<sub>3</sub> nanoparticles, *Sens. Actuators B* 131 (2008) 183–189.
- [6] C.M. Ghimbeu, M. Lumbrebras, M. Siadat, R.C. van Landschoot, J. Schoonman, Electrostatic sprayed SnO<sub>2</sub> and Cu-doped SnO<sub>2</sub> films for H<sub>2</sub>S detection, *Sens. Actuators B* 133 (2008) 694–698.
- [7] Z. Zeng, K. Wang, Z. Zhang, J. Chen, W. Zhou, The detection of H<sub>2</sub>S at room temperature by using individual indium oxide nanowire transistors, *Nanotechnology* 20 (2009) 045503 (4 pp.).
- [8] Y. Shen, T. Yamazaki, Z. Liu, D. Meng, T. Kikuta, N. Nakatani, M. Saito, M. Mori, Microstructure and H<sub>2</sub> gas sensing properties of undoped and Pd-doped SnO<sub>2</sub> nanowires, *Sens. Actuators B* 135 (2009) 524–529.
- [9] E. Comini, G. Faglia, G. Sberveglieri, D. Calestani, L. Zanotti, M. Zha, Tin oxide nanobelts electrical and sensing properties, *Sens. Actuators B* 111–112 (2005) 2–6.
- [10] M.R. Yang, S.Y. Chu, R.C. Chang, Synthesis and study of the SnO<sub>2</sub> nanowires growth, *Sens. Actuators B* 122 (2007) 269–273.
- [11] S.H. Luo, J.Y. Fan, W.L. Liu, M. Zhang, Z.T. Song, C.L. Lin, X.L. Wu, P.K. Chu, Synthesis and low-temperature photoluminescence properties of SnO<sub>2</sub> nanowires and nanobelts, *Nanotechnology* 17 (2006) 1695–1699.
- [12] J.Q. Hu, Y. Bando, D. Golberg, Self-catalyst growth and optical properties of novel SnO<sub>2</sub> fishbone-like nanoribbons, *Chem. Phys. Lett.* 372 (2003) 758–762.
- [13] N. Dharmaraj, C.H. Kim, K.W. Kim, H.Y. Kim, E.K. Suh, Spectral studies of SnO<sub>2</sub> nanofibers prepared by electrospinning method, *Spectrochim. Acta A* 64 (2006) 136–140.
- [14] D. Wang, X.F. Chu, M.L. Gong, Gas-sensing properties of sensors based on single-crystalline SnO<sub>2</sub> nanorods prepared by a simple molten-salt method, *Sens. Actuators B* 117 (2006) 183–187.
- [15] G. Otulakowski, B.P. Kavanagh, Hydrogen sulfide in lung injury: therapeutic hope for a toxic gas? *Anesthesiology* 113 (2010) 4–6.
- [16] D. Vuong, G. Sakai, K. Shimano, N. Yamazoe, Hydrogen sulfide gas sensing properties of thin films derived from SnO<sub>2</sub> sols different in grain size, *Sens. Actuators B* 105 (2005) 437–442.
- [17] I. S. Hwang, J.K. Choi, S.J. Kim, K.Y. Dong, J.H. Kwon, B.K. Ju, J.H. Lee, Enhanced H<sub>2</sub>S sensing characteristics of SnO<sub>2</sub> nanowires functionalized with CuO, *Sens. Actuators B* 142 (2009) 105–110.
- [18] J. Xu, X. Wang, J. Shen, Hydrothermal synthesis of In<sub>2</sub>O<sub>3</sub> for detecting H<sub>2</sub>S in air, *Sens. Actuators B* 115 (2006) 642–646.
- [19] J.K. Choi, I.S. Hwang, S.J. Kim, J.S. Park, S.S. Park, U. Jeong, Y.C. Kang, J.H. Lee, Design of selective gas sensors using electrospun Pd-doped SnO<sub>2</sub> hollow nanofibers, *Sens. Actuators B* 150 (2010) 191–199.
- [20] Q. Wan, Q.H. Li, Y.J. Chen, T.H. Wang, X.L. He, X.G. Gao, J.P. Li, Positive temperature coefficient resistance and humidity sensing properties of Cd-doped ZnO nanowires, *Appl. Phys. Lett.* 84 (2004) 3082.
- [21] Q. Wan, Q.H. Li, Y.J. Chen, T.H. Wang, X.L. He, J.P. Li, C.L. Lin, Fabrication and ethanol sensing characteristics of ZnO nanowire gas sensors, *Appl. Phys. Lett.* 84 (2004) 3654.
- [22] W.P. Kang, C.K. Kim, Performance analysis of a new metal-insulator-semiconductor capacitor incorporated with Pt-SnO<sub>x</sub> catalytic layers for the detection of O<sub>2</sub> and Co gases, *J. Appl. Phys.* 75 (1994) 4237–4242.
- [23] A. Cabot, J. Arbiol, J.R. Morante, U. Weimar, N. Barsan, W. Gopel, Analysis of the noble metal catalytic additives introduced by impregnation of as obtained SnO<sub>2</sub> sol-gel nanocrystals for gas sensors, *Sens. Actuators B* 70 (2000) 87–100.
- [24] N. Yamazoe, New approaches for improving semiconductor gas sensors, *Sens. Actuators B* 5 (1991) 7–19.
- [25] M.V. Vaishampayan, R.G. Deshmukh, P. Walke, I.S. Mulla, Fe-doped SnO<sub>2</sub> nanomaterial: a low temperature hydrogen sulfide gas sensor, *Mater. Chem. Phys.* 109 (2008) 230–234.
- [26] S. Seal, S. Shukla, Nanocrystalline SnO gas sensors in view of surface reactions and modifications, *JOM* 54 (2002) 35–38.
- [27] M. Kaur, S. Bhattacharya, M. Roy, S.K. Deshpande, P. Sharma, S.K. Gupta, J.V. Yakhmi, Growth of nanostructures of Zn/ZnO by thermal evaporation and their application for room-temperature sensing of H<sub>2</sub>S gas, *Appl. Phys. A* 87 (2007) 91–96.

#### Biographies

**Ki-Young Dong** received his MS degree at Korea University in 2009. Currently, he is a Ph.D. candidate in the Department of Electrical Engineering, Korea University. His research interests are nano material based gas sensors and nano patterning technology.

**Joong-Ki Choi** studied materials science and engineering and received his BS degree from Korea University in 2009. He is currently a master course student at Korea University. His research topic is oxide nanofiber gas sensors.



**In-Sung Hwang** studied materials science and engineering and received his BS from Kumoh National University, Korea, in 2004. In 2006, he received his MS degree from Korea University. He is currently studying for a Ph. D at Korea University. His research interest is oxide nanostructure-based electronic devices.

**Jin-Woo Lee** received his PhD degree from the Department of Materials Science, Seoul National University in 1999. He worked at the Max-Planck Institute for micro-structural physics, Germany and at Watter-Schottky Institute of Techniscal University of Munich, Germany.

**Byung Hyun Kang** received his MS degree at Korea University in 2004. Currently, he is a Ph.D. candidate in the Department of Electrical Engineering, Korea University. His research interests are graphene based nano devices.

**Dae-Jin Ham** received his BS degree from the Department of Electrical Engineering, Inha University in 2009. He is currently a master course student at Korea University. His research topic is chemical sensors.

**Jong-Heun Lee** has been a Professor at Korea University since 2008. He received his BS, MS, and Ph.D. degrees from Seoul National University in 1987, 1989, and

1993, respectively. Between 1993 and 1999, he developed automotive air-fuel-ratio sensors at the Samsung Advanced Institute of Technology. He was a Science and Technology Agency of Japan (STA) fellow at the National Institute for Research in Inorganic Materials (currently NIMS, Japan) from 1999 to 2000, a research professor at Seoul National University from 2000 to 2003, and an associate professor at Korea University from 2003 to 2008. His current research interests include chemical sensors, functional nanostructures, and solid oxide electrolytes.

**Byeong-Kwon Ju** received his ME in electronics engineering from the University of Seoul in 1988 and a PhD in semiconductor engineering from Korea University in 1995. In 1988, he joined the Korea Institute of Science and Technology (KIST), Seoul, where he was mainly engaged in the development of silicon micromachining and microsensors as a principal research scientist. In 1996, he spent 6 months as a visiting research fellow at the Microelectronics Centre, University of South Australia, Australia. Since 2005, he has been an associate professor of Korea University with his main interest in flexible electronics (OLED, OTFT), field emission devices, MEMS (Bio and RF) and carbon nanotube-based nanosystems.